

Regulation of the Physical Characteristics of Titania Nanotube Aggregates Synthesized from Hydrothermal Treatment

Chien-Cheng Tsai and Hsisheng Teng*

Department of Chemical Engineering and NCU-ITRI Joint Research Center, National Cheng Kung University, Tainan 70101, Taiwan

Received March 2, 2004. Revised Manuscript Received June 1, 2004

Titania nanotube aggregates with different porosities were prepared from hydrothermal treatment on commercial TiO_2 particles in NaOH followed by HCl washing. Pore structure analysis reflects that pores of smaller sizes are mainly contributed by the nanotubes while those of larger sizes are contributed by the interspace region of the aggregates. The hydrothermal treatment temperature, ranging within 110–150 °C, was shown to affect not only the extent of particle-to-sheet conversion, and thus the resulting structures of the nanotubes, but also the anatase-to-rutile transformation at high temperatures. The surface area of the nanotube aggregates increases with the treatment temperature to reach a maximum of ca. 400 m^2/g at 130 °C, and then decreases with further increase of the temperature. In HCl washing, both the charge-removal rate and final state of the electrostatic charges on TiO_2 affect the rolling of TiO_2 sheets into nanotubes. This demonstrates that the nanotube structure can be regulated by adjusting the washing condition. Selective catalytic reduction of NO with NH_3 has been conducted to prove that the vast surface of the nanotube aggregates is accessible to the interacting molecules.

Introduction

Titania (or TiO_2), a wide band gap semiconductor, can generate powerful oxidants (valence-band holes) and reductants (conduction-band electrons) by absorbing photon energies.^{1–3} Because of this feature and its durability, TiO_2 has been extensively studied for applications in photoelectrochemical systems, such as dye-sensitized TiO_2 electrodes for photovoltaic solar cells and water-splitting catalysts for hydrogen generation.^{4–6} In addition to the photon-related processes, TiO_2 also has many important applications as a conventional catalyst or support of catalysts for the elimination of pollutants in gas or liquid phases.^{7,8}

In all the applications mentioned above, the structure of TiO_2 employed must have sufficiently high surface area for interaction and optimum pore size to allow diffusion of active species. Therefore, how to enlarge the surface area and control the pore size are important issues for the application of TiO_2 . In addition to the pore

structure, the performance of TiO_2 also depends on its crystalline phase, particle size, and crystallinity.^{2,5} TiO_2 has three crystalline phases—anatase, rutile, and brookite—which own different band gap energies and chemical activities. An increase in crystallinity has been reported to result in an activity promotion.²

Recently, preparation of TiO_2 nanotubes from hydrothermal treatment with alkali solutions,^{9–18} deposition with templates,^{19–23} or anodic oxidation of titanium^{24,25} have been reported, and the products have been exten-

* To whom correspondence should be addressed. Tel: 886-6-2385371. Fax: 886-6-2344496. E-mail: hteng@mail.ncku.edu.tw.

(1) Hoffman, M. R.; Martin, S. T.; Choi, W.; Bahnemann, D. W. *Chem. Rev.* **1995**, *95*, 69.

(2) Stone, V. F.; Davis, R. J. *Chem. Mater.* **1998**, *10*, 1468.

(3) Adachi, M.; Murata, Y.; Harada, M.; Yoshikawa, S. *Chem. Lett.* **2000**, *942*.

(4) O'Regan, B.; Grätzel, M. *Nature* **1991**, *353*, 737.

(5) Park, N. G.; Lagemaat, J.; Frank, A. J. *J. Phys. Chem. B* **2000**, *104*, 8989.

(6) Khan, S. U. M.; Al-Shahry, M.; Ingler, W. B. *Science* **2002**, *297*, 2243.

(7) Komova, O. V.; Simakov, A. V.; Rogov, V. A.; Kochubei, D. I.; Odegova, G. V.; Kriventsov, V. V.; Paukshtis, E. A.; Ushakov, V. A.; Sazonova, N. N.; Nikoro, T. A. *J. Mol. Catal. A* **2000**, *161*, 191.

(8) Qi, G.; Yang, R. T. *Appl. Catal. B* **2003**, *44*, 217.

(9) Kasuga, T.; Hiramatsu, M.; Hoson, A.; Sekino, T.; Niihara, K. *Langmuir* **1998**, *14*, 3160.

(10) Kasuga, T.; Hiramatsu, M.; Hoson, A.; Sekino, T.; Niihara, K. *Adv. Mater.* **1999**, *11*, 1307.

(11) Du, G. H.; Chen, Q.; Che, R. C.; Yuan, Z. Y.; Peng, L. M. *Appl. Phys. Lett.* **2001**, *79*, 3702.

(12) Seo, D. S.; Lee, J. K.; Kim, H. J. *Cryst. Growth* **2001**, *229*, 428.

(13) Zhu, Y.; Li, H.; Koltypin, Y.; Hacohen, Y. R.; Gedanken, A. *Chem. Commun.* **2001**, 2616.

(14) Yuan, Z. Y.; Zhou, W.; Su, B. L. *Chem. Commun.* **2002**, 1202.

(15) Chen, Q.; Du, G. H.; Zhang, S.; Peng, L. M. *Acta Crystallogr., Sect. B* **2002**, *58*, 587.

(16) Zhang, Q.; Gao, L.; Sun, J.; Zheng, S. *Chem. Lett.* **2002**, 226.

(17) Wang, Y. Q.; Hu, G. Q.; Duan, X. F.; Sun, H. L.; Xue, Q. K. *Chem. Phys. Lett.* **2002**, *365*, 427.

(18) Tian, Z. R.; Voigt, J. A.; Liu, J.; McKenzie, B.; Xu, H. *J. Am. Chem. Soc.* **2003**, *125*, 12384.

(19) Hoyer, P. *Langmuir* **1996**, *12*, 1411.

(20) Imai, H.; Takei, Y.; Shimizu, K.; Matsuda, M.; Hirashima, H. *J. Mater. Chem.* **1999**, *9*, 2971.

(21) Lei, Y.; Zhang, L. D.; Meng, G. W.; Li, G. H.; Zhang, X. Y.; Liang, C. H.; Chen, W.; Wang, S. X. *Appl. Phys. Lett.* **2001**, *78*, 1125.

(22) Michailowski, A.; AlMawlawi, D.; Cheng, G.; Moskovits, M. *Chem. Phys. Lett.* **2001**, *349*, 1.

(23) Liu, S. M.; Gan, L. M.; Liu, L. H.; Zhang, W. D.; Zeng, H. C. *Chem. Mater.* **2002**, *14*, 1391.

(24) Gong, D.; Grimes, C. A.; Varghese, O. K. *J. Mater. Res.* **2001**, *16*, 3331.

(25) Varghese, O. K.; Gong, D.; Paulose, M.; Grimes, C. A.; Dickey, E. C. *J. Mater. Res.* **2003**, *18*, 156.

sively studied. TiO_2 in the form of nanotubes is expected to have larger specific surface area and pore volume in comparison with that in the form of nanoparticles. Hydrothermal treatment with alkali solutions is of particular interest because nanotube aggregates can be produced in an unsophisticated manner at low temperatures. In the present work, the influence of the hydrothermal treatment condition on the properties of nanotube products will be examined. Owing to the considerably low structural stability of TiO_2 at high temperatures,²⁵ how the pore structure and crystalline phase of the TiO_2 nanotube aggregates would vary with subsequent calcination is an important issue for future applications and will be investigated here as well. The obtained results concerning the effects of preparation parameters can be employed to regulate the physical characteristics of the nanotube aggregates. The high-surface-area advantage of nanotubes in reaction will be examined by NO reduction with NH_3 , using TiO_2 as the catalyst support.

Experimental Section

The TiO_2 source used for nanotube production was commercial-grade TiO_2 powder (P25, Degussa AG, Germany) with crystalline structure of ca. 30% rutile and 70% anatase and primary particle size of ca. 21 nm. In nanotube preparation, 2 g of the TiO_2 powder was mixed with 70 mL of 10 N NaOH solution, followed by thermal treatment of the mixture at 110–150 °C in a Teflon-lined autoclave for 24 h. After the treatment, the filtered sample was then neutralized by mixing with 1 L of 0.1 N HCl solution for several times until the pH value of the rinsing solution was less than 7. The powder was dried at 100 °C for 3 h to give the as-synthesized nanotube product. To explore the thermal stability, the as-synthesized nanotubes were calcined at different temperatures for 1 h.

The phase identification and structural analysis of the TiO_2 samples at different stages of preparation and treatment was conducted with powder X-ray diffraction (XRD) using a Rigaku RINT2000 diffractometer equipped with Cu K α radiation. The data were collected for scattering angles (2θ) ranging between 20 and 70° with a step size of 0.01°. The external features and morphology of the TiO_2 were analyzed by using a high-resolution transmission electron microscope (HR-TEM, Hitachi FE-2000).

Pore structure of the derived TiO_2 nanotubes was characterized by N_2 adsorption at –196 °C using an adsorption apparatus (Micromeritics, ASAP 2010). Surface area of the samples was determined from the Brunauer–Emmett–Teller (BET) equation and pore volume from the total amount adsorbed at relative pressures near unity. The pore size distribution was analyzed by using the Barrett–Joyner–Halenda (BJH) method.

The high-porosity advantage of the TiO_2 nanotubes serving as a catalyst support was examined in selective catalytic reduction (SCR) of NO with NH_3 , using Cu as the active species. For the purpose of comparison, P25 as well as the nanotube sample was impregnated with Cu using $\text{Cu}(\text{NO}_3)_2$ solution. The incipient-wetness impregnation of Cu was conducted and followed by vacuum-drying at 110 °C for 24 h. The Cu-impregnated samples were then heated at 350 °C in helium for 2 h to remove the residual nitrates. The Cu content was controlled to 1 wt %.

The SCR experiments were performed over a fixed bed containing 0.2 g of catalyst particles. At the atmospheric pressure reactant gases—640 ppm NO, 640 ppm NH_3 , and 1 vol. % O_2 —were fed to the reactor through mass flow controllers, with addition of helium to make up a total flow rate of 300 cm^3/min . The NO concentration was analyzed by a chemiluminescence NO/NO_x analyzer. The reaction temperature ranged between 100 and 400 °C.

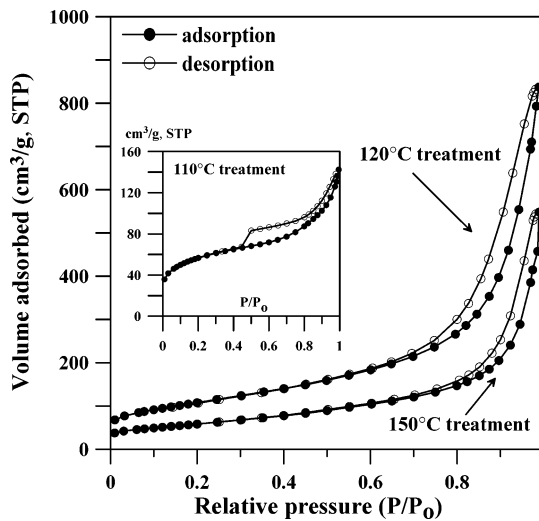


Figure 1. N_2 adsorption isotherms at –196 °C for TiO_2 nanotube aggregates from hydrothermal treatment in NaOH at 110 (the insert), 120, and 150 °C. The treatment was followed by washing several times with 1 L of 0.1 N HCl until pH < 7 reached.

Table 1. Pore Structures of TiO_2 Nanotube Aggregates from Hydrothermal Treatment in NaOH at Different Temperatures^a

| hydrothermal treatment temperature (°C) | S_{BET} (m ² /g) | V_{total} (cm ³ /g) | peak pore size ^b (nm) |
|---|--------------------------------------|---|----------------------------------|
| 110 | 207 | 0.24 | 3.8 |
| 120 | 245 | 1.41 | 20.9 |
| 130 | 399 | 1.47 | 18.1 |
| 140 | 348 | 1.18 | 18.5 |
| 150 | 209 | 0.84 | 31.1 |

^a The treatment was followed by washing several times with 1 L of 0.1 N HCl until pH < 7 was reached. ^b Peak position in the BJH pore size distribution.

Results and Discussion

Figure 1 shows the typical isotherms of N_2 adsorption onto the nanotube products from hydrothermal treatment in NaOH at 120 and 150 °C. These isotherms exhibit obvious hysteresis behavior, indicating that the products are mainly mesoporous.²⁶ The pore structures calculated according to the adsorption data are summarized in Table 1. In most cases, the specific surface areas are high in comparison with the starting material P25, which has a surface area of ca. 50 m²/g. The surface area increases with the synthesis temperature (i.e., the hydrothermal treatment temperature) to reach a maximum of 399 m²/g at 130 °C, and then decreases with further temperature increase. Nanotubes with high surface area prepared from hydrothermal treatment using different TiO_2 sources have been reported.^{9,12,14,16} Table 2 summarizes the results of the previous studies. Basically, TiO_2 nanoparticles derived from sol–gel or hydrolysis methods were employed as the starting materials. The resulting nanotubes exhibited surface areas in a range of 100–450 m²/g. Comparing the data in Tables 1 and 2 reflects that the nanotube aggregates obtained from the commercial nanoparticle P25 in the present work have surface areas similar to those

Table 2. Preparation Conditions and Surface Areas of TiO₂ Nanotube Products Reported in the Literature

| TiO ₂ source | hydrothermal treatment condition | rinsing solution | S _{BET} (m ² /g) | ref |
|---|-----------------------------------|------------------|--------------------------------------|----------------------------|
| nanoparticles from Ti-(O-C ₃ H ₇) ₄ using sol-gel method; S _{BET} = 150 m ² /g | 2.5–20 N NaOH; 20–110 °C for 20 h | 0.1 N HCl | ca. 400 | Kasuga et al. ⁹ |
| nanoparticles from precipitates by dropping NH ₄ OH into TiOCl ₂ ; S _{BET} = 160 m ² /g | 5 N NaOH; 100–200 °C for 12 h | water | 180–270 | Seo et al. ¹² |
| nanoparticles from Ti-(O-C ₃ H ₇) ₄ using sol-gel method; no S _{BET} available | 5–15 N NaOH; 100–180 °C for 48 h | 0.1 N HCl | 267–375 | Yuan et al. ¹⁴ |
| nanoparticles from precipitates by dropping (NH ₄) ₂ SO ₄ or HCl into TiCl ₄ , with subsequent NH ₄ OH neutralization; S _{BET} = 5–290 m ² /g | 10 N NaOH; 110 °C for 20 h | 0.1 N HCl | 107–451 | Zhang et al. ¹⁶ |
| nanoparticles P25 of commercial Degussa AG, from hydrolysis of TiCl ₄ in a H ₂ /O ₂ flame; S _{BET} = 50 m ² /g | 10 N NaOH; 110–150 °C for 24 h | 0.1 N HCl | 200–400 | present work |

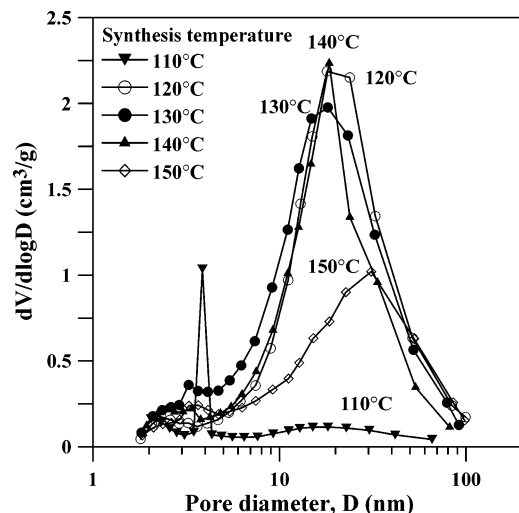


Figure 2. Pore size distributions of TiO₂ nanotube aggregates from hydrothermal treatment in NaOH at different temperatures. The treatment was followed by washing several times with 1 L of 0.1 N HCl until pH < 7 reached.

reported previously. Since the morphology of TiO₂ nanotubes strongly depends on the size and crystalline phase of the TiO₂ source,¹⁶ use of the standardized P25 as the starting material has the advantage in the property control of the nanotube products for subsequent application or even mass production.

An auxiliary experiment shows that, prior to the acid neutralization, 30 min of stirring of the mixture from the hydrothermal treatment was able to enhance the surface area. With this stirring process, the surface area of the 130 °C-synthesized sample was increased to ca. 430 m²/g. The reason for this surface area enhancement is not clear, and the stirring was not executed in the present work unless otherwise indicated.

As for the pore volume shown in Table 1, the maximum value occurs at 130 °C as well. However, the pore volume of the 120 °C-synthesized sample is similar to that of the 130 °C-synthesized sample, while the surface area is significantly smaller. This difference suggests that the tube diameter of the sample from 120 °C synthesis is larger than that from 130 °C. The BJH method was employed to analyze the pore size distributions and the results are shown in Figure 2. The distributions are relatively wide, ranging between 2 and 100 nm. The peak positions of the pore size distributions

for the samples synthesized at different temperatures are listed in Table 1. It indeed shows that the peak pore size is larger for 120 °C treatment than for 130 °C. The increase in surface area or pore volume with the hydrothermal treatment temperature in the low-temperature regime (<130 °C) can be attributed to the enhanced rupture of Ti–O–Ti bonds in the nanoparticles to form Ti–O–Na and Ti–OH.^{9,14} The rupture leads to the formation of lamellar TiO₂ sheets because of the electrostatic repulsion of the charge on sodium.⁹ The sheets would scroll to become nanotubes after HCl washing. Figure 3a shows the TEM image of the titania after hydrothermal treatment at 130 °C. Titania in the form of lamellar sheets can be seen. Nanotubes are formed after treating the sheets with HCl, as confirmed by the TEM image in Figure 3b. The tube size, judged from the TEM image, ranges between 10 and 30 nm, in agreement with the results evaluated from the BJH method. In the case of 110 °C treatment, the N₂ adsorption–desorption isotherm branches of the resulting product (see the insert in Figure 1) were found to be typical of the H3-type hysteresis loops in IUPAC classification.²⁶ This indicates that the TiO₂ product consists of platelike particles. Treatment at 110 °C may only result in a low extent of bond rupture, forming plates thicker than the lamellar sheets obtained at higher treatment temperatures. These plates cannot scroll to become nanotubes after HCl washing. The peak pore size of ca. 4 nm in the BJH analysis may represent the average interval between the platelike particles.

For the hydrothermal treatment at temperatures higher than 130 °C, the surface area and pore volume of the products decrease with the temperature. The pore size distribution in Figure 2 reflects that the pore volume decrease with temperature mainly results from the loss of pores of smaller sizes. It is possible that the extensive treatment at high temperatures causes the destruction of the lamellar TiO₂. Thus, a significant amount of granular particles (observed from scanning electron microscopy), in addition to nanotubes, are obtained with the subsequent charge removal by HCl washing, leading to the reduction in the porosity of the resulting products. The volume of larger pores remaining does not change with high temperature treatment and may be mainly contributed by the interspace region of the aggregates.

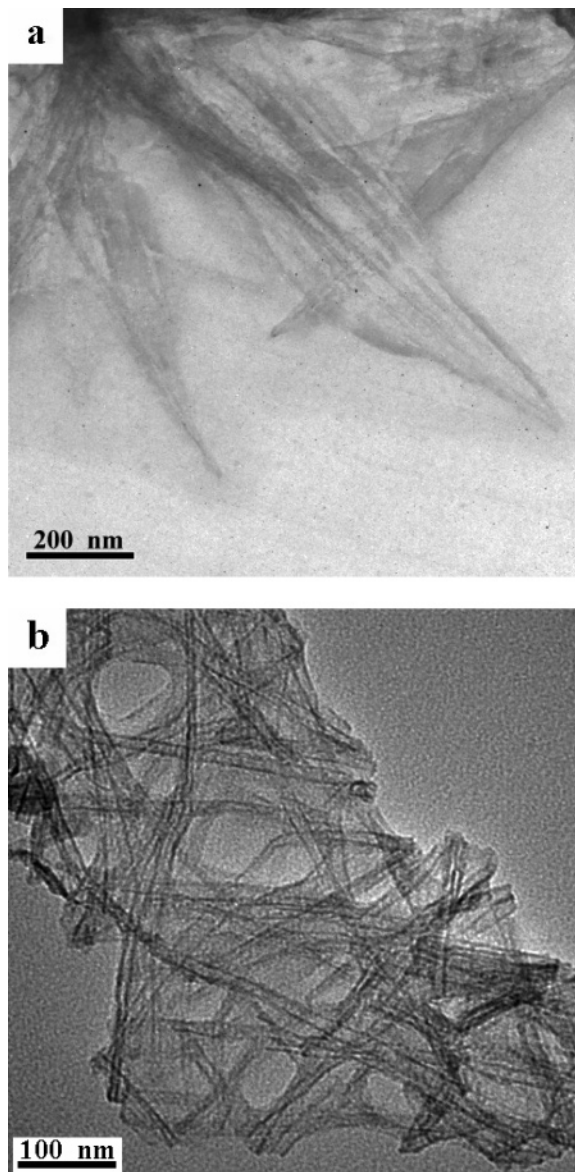


Figure 3. TEM images of TiO_2 from (a) hydrothermal treatment in NaOH at $130\text{ }^\circ\text{C}$; and (b) the hydrothermal treatment with subsequent HCl washing.

Because of the high surface area, these TiO_2 nanotubes will attract interest in catalysis. In many practical applications the reaction temperatures are higher than the ambient, and thus the thermal stability of the catalysts used has to be taken into account. The high-temperature structural stability of the TiO_2 nanotube aggregates was examined by calcination at different temperatures for 1 h. The variation of the surface area with the calcination temperature is shown in Figure 4. The surface area decreases sharply with the temperature, indicating sintering of the tubes upon thermal treatment. Products from calcination at temperatures higher than $600\text{ }^\circ\text{C}$ have surface areas lower than the precursor P25. This indicates that the high-porosity advantage of the nanotube aggregates over P25 is preserved only for reactions conducted at temperatures lower than $600\text{ }^\circ\text{C}$. Figure 5 shows the TEM images of the $130\text{ }^\circ\text{C}$ -synthesized nanotubes calcined at $400\text{ }^\circ\text{C}$ and higher temperatures. With calcination at $400\text{ }^\circ\text{C}$ the products remain tube-like. Further increase of the temperature to $600\text{ }^\circ\text{C}$ results in sintering of the tubes

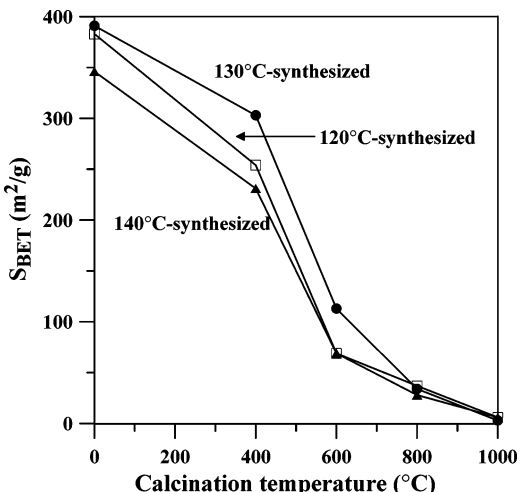


Figure 4. BET surface areas of the TiO_2 nanotube aggregates calcined at different temperatures. The nanotube aggregates were synthesized in NaOH at different temperatures, followed by washing several times with 1 L of 0.1 N HCl until $\text{pH} < 7$ reached.

to form rodlike structures. The sintering is accompanied by an abrupt decrease in surface area, as shown in Figure 4. Figure 5c shows that the rodlike TiO_2 agglomerates at $800\text{ }^\circ\text{C}$, forming cylindrical particles of larger sizes.

Apart from pore structure, the crystalline structure of TiO_2 should also be considered for its applications. Figure 6 shows the XRD patterns of the $130\text{ }^\circ\text{C}$ -synthesized nanotubes calcined at different temperatures. The data for the precursor P25 are also provided, showing the presence of both anatase and rutile phases. The representative peaks are the anatase [101] diffraction at a scattering angle (2θ) of 25.28° and the rutile [110] at 27.44° . The as-synthesized nanotubes show vague peaks in the anatase phase. The anatase phase (with a longer c axis) has been reported to be the preferred phase in TiO_2 nanotubes.¹⁶ Obviously, the hydrothermal treatment converts the rutile in P25 to anatase. The vague peaks indicate the small number of crystalline layers due to the small wall thickness of the tubes. Upon calcination the anatase crystalline domains became enlarged, according to the sharpening appearance of the anatase peaks. For calcination at temperatures above $900\text{ }^\circ\text{C}$, transformation of the metastable anatase phase to the stable rutile phase can be observed.

The onset temperature for the anatase-to-rutile was found to vary with the temperature for nanotube synthesis. Figure 7 shows that the phase-transformation temperature increases with the synthesis temperature and levels off at synthesis temperatures above $130\text{ }^\circ\text{C}$. For synthesis at temperatures lower than $130\text{ }^\circ\text{C}$, it appears that the phase-transformation temperature increases with the surface area of the nanotube aggregates. Because the anatase is feasible for nanotubes formation,¹⁶ the high surface area of the sample from $130\text{ }^\circ\text{C}$ synthesis suggests the high proportion of anatase phase in the structure. For synthesis temperatures lower than $130\text{ }^\circ\text{C}$, there would be the presence of unconverted rutile, thus resulting in lower surface areas. It has been reported that the growth of rutile involves interactions between the existing rutile par-

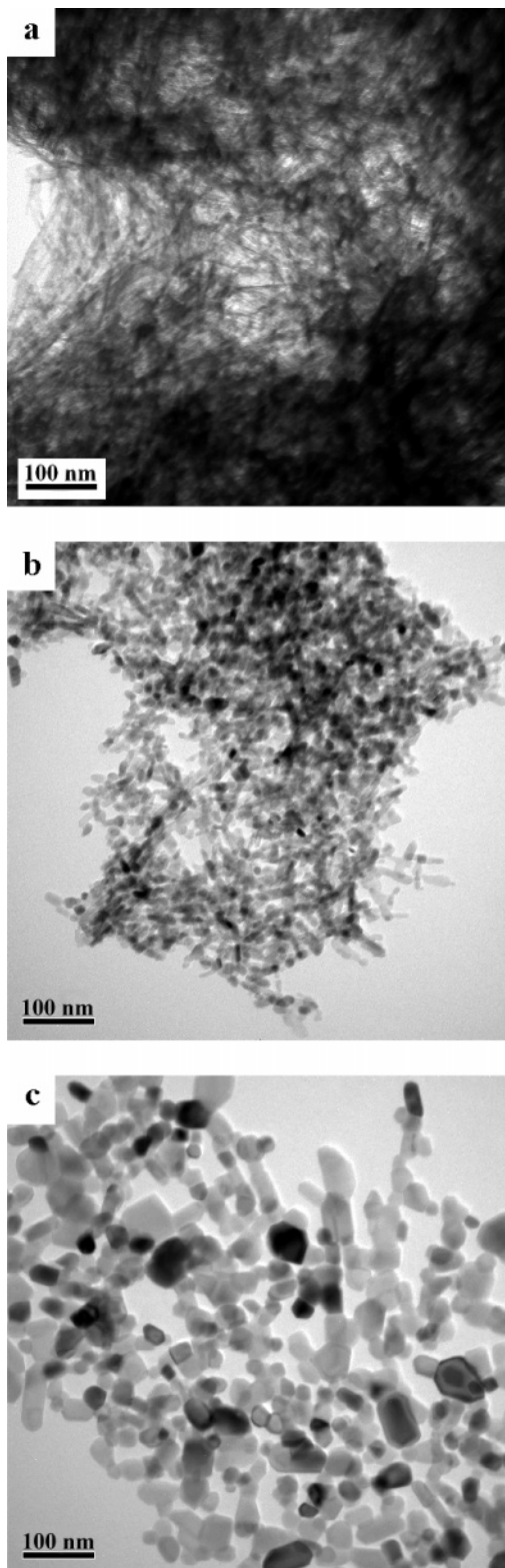


Figure 5. TEM images of the TiO_2 nanotube aggregates calcined at different temperatures: (a.) 400 $^{\circ}\text{C}$; (b) 600 $^{\circ}\text{C}$; and (c) 800 $^{\circ}\text{C}$. The nanotube aggregates were synthesized in NaOH at 130 $^{\circ}\text{C}$, followed by washing several times with 1 L of 0.1 N HCl until pH <7 was reached.

ticles and the surrounding anatase particles.²⁷ This suggests that the rutile present in the nanotubes synthesized at lower temperatures would accelerate the

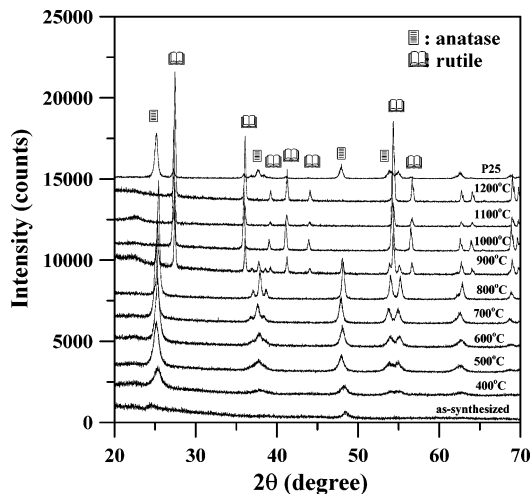


Figure 6. XRD patterns of P25 and the TiO_2 nanotube aggregates calcined at different temperatures. The nanotube aggregates were synthesized in NaOH at 130 $^{\circ}\text{C}$, followed by washing several times with 1 L of 0.1 N HCl until pH <7 was reached.

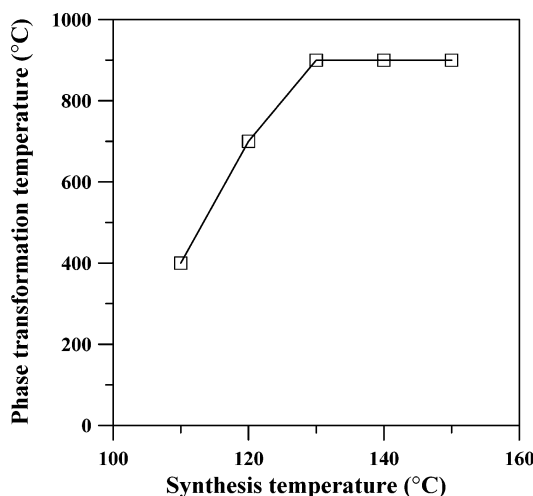


Figure 7. Variation of the anatase-to-rutile transformation temperature with the synthesis temperature for the nanotube aggregates synthesized in NaOH, followed by washing several times with 1 L of 0.1 N HCl until pH <7 was reached.

growth of rutile, thus leading to a lower temperature for anatase-to-rutile transformation. On the other hand, synthesis at 130 $^{\circ}\text{C}$ has reached the saturation of the anatase phase and a further increase of the temperature would not affect the thermal stability of the anatase, as reflected in Figure 7. Auxiliary XRD measurements have shown that for nanotubes synthesized at temperatures higher than 120 $^{\circ}\text{C}$ there are vague, but identifiable, anatase-phase peaks observed with their intensity increasing slightly with the synthesis temperature, while no identifiable peaks appear for those synthesized at lower temperatures. This may partially support the above argument that the increase in the anatase phase of the nanotubes would result in an elevation of the onset temperature for anatase-to-rutile transformation.

It has been shown that in nanotube preparation acid treatment removes the electrostatic repulsion and results in the formation of TiO_2 nanotubes from lamellar sheets. This nanotube-formation mechanism suggests that the extent of acid treatment may become the key factor determining how the sheets scroll and thus the

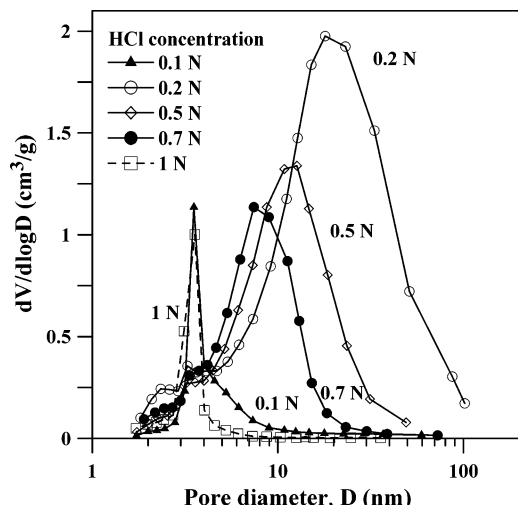


Figure 8. Pore size distributions of TiO_2 nanotube aggregates from rinsing with HCl solutions of different concentrations. Before rinsing, the hydrothermal treatment in NaOH was conducted at 130°C .

Table 3. Pore Structures of the 130°C -Synthesized TiO_2 Nanotube Aggregates Obtained by Rinsing with HCl Solutions of Different Concentrations

| HCl concn (N) | S_{BET} (m^2/g) | V_{total} (cm^3/g) | peak pore size ^a (nm) | pH value of the mixture |
|---------------|--|---|----------------------------------|-------------------------|
| 0.1 | 119 | 0.18 | 3.5 | 12 |
| 0.2 | 397 | 1.54 | 21.8 | 1.6 |
| 0.5 | 270 | 0.8 | 12.7 | 0.87 |
| 0.7 | 296 | 0.56 | 7.4 | 0.62 |
| 1 | 94 | 0.12 | 3.6 | 0.38 |

^a Peak position in the BJH pore size distribution.

overall pore structure of the resulting aggregates. Instead of the repeated washing with 0.1 N HCl, the sample hydrothermally treated at 130°C was subjected to neutralization with 1 L of HCl solutions of 0.1–1 N in concentration. Table 3 shows the pore structures of the TiO_2 nanotube aggregates from washing with different HCl concentrations. The equilibrium pH values of the TiO_2 -solution mixtures are also listed in Table 3, showing that the pH value is a decreasing function of HCl concentration. The pore structure data reveal that the porosity increases with the HCl concentration and reaches its maximum at 0.2 N HCl, at which the equilibrium pH value is 1.6. With further increasing the HCl concentration, the porosity is found to decrease. The pore size distributions of these nanotube aggregates are shown in Figure 8 and the peak positions of the distribution are listed in Table 3. It is of interest to see that the peak pore size increases with the HCl concentration, from 3.5 nm at 0.1 N to a maximum of 21.8 nm at 0.2 N. With a HCl concentration of 0.1 N, the N_2 adsorption–desorption branches of the resulting product were found to be close to the H3 hysteresis loops. This indicates that the lamellar TiO_2 cannot scroll to tubes in a basic environment (with a pH value as high as 12), resulting in a low surface area of the product. Obviously, an acidic environment is necessary for the formation of the nanotubes. Above 0.2 N, the peak pore size decreases with the increase in the concentration. The tube size decrease with the HCl concentration can be attributed to the dynamic reason; i.e., rapid removal of electrostatic charges leads to the folding of the sheets

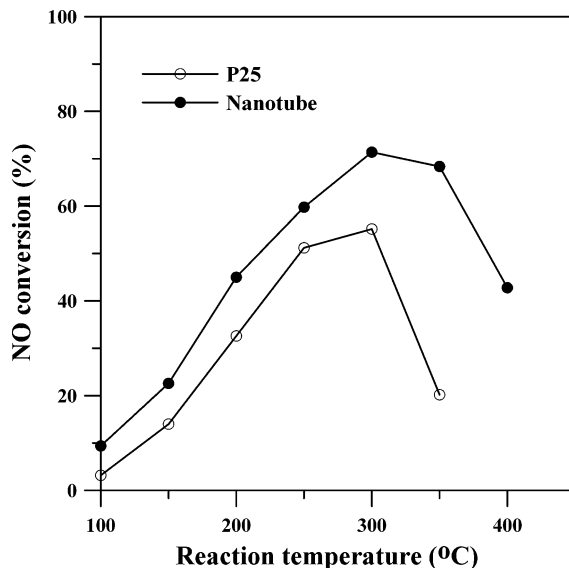


Figure 9. Variation of steady-state NO conversion with temperature for reactions over the 130°C -synthesized nanotube and P25 nanoparticle samples impregnated with 1 wt % of Cu. The nanotubes were obtained with washing several times with 1 L of 0.1 N HCl until pH <7 reached, followed by calcination at 400°C .

to become granules, instead of tubes.⁹ The isotherm hysteresis of the 1-N-HCl-washed products was found to be of the H2-type, which is characteristic of corpuscular systems. This confirms that the products from concentrated-HCl washing consists of granules, rather than tubes.

The above interpretation suggests that the final structure of TiO_2 aggregates is significantly controlled by dynamics. Nevertheless, the influence of the equilibrated electrostatic charge on TiO_2 should also be taken into account. To examine this, a sequence of HCl treatment, 0.2 N followed by 1 N, was conducted, and the product was subjected to pore analysis. The surface area and peak size of the TiO_2 sample were found to be $219 \text{ m}^2/\text{g}$ and 6.4 nm , respectively. Both values are smaller than those of the 0.2-N-rinsed sample, but larger than those of the 1-N-rinsed sample. The results reflect that the process for nanotube formation is controlled by the charge-removing rate as well as the final number of electrostatic charges on the sheets. Another rinsing sequence—1 N HCl, 1 N NaOH, and finally 0.2 N HCl—was employed, and the product was found to have a surface area of $317 \text{ m}^2/\text{g}$ and a peak size of 15.1 nm . The structure seems to be partially reversible with the equilibrium state of the mixture. The results confirm our argument that both the charge-removing rate and equilibrium condition of the electrostatic charges are important factors affecting the pore structures of the nanotube aggregates.

To examine the accessibility of the nanotube surface to reacting molecules, nanotube aggregates were subjected to 1 wt % Cu impregnation and then catalytic activity measurements in SCR. The aggregates used were the 130°C -synthesized sample in Table 1 with subsequent calcination at 400°C . The starting material P25 was also tested for the purpose of comparison. The temperature dependence of the steady-state NO conversion over these catalysts is shown in Figure 9. It can be seen that the nanotube sample exhibits a high activity

than the nanoparticle P25. The difference in the surface areas, 303 and 50 m²/g for the nanotube and nanoparticle samples, respectively, can at least partially explain the higher activity of the nanotube sample. An auxiliary temperature-programmed reduction experiment has shown that the reduction signal for copper oxides over the nanotubes is larger than that over the P25, an indication of higher dispersion of Cu over the nanotubes.

Summary and Conclusions

The present work has demonstrated that the pore structures of TiO₂ nanotube aggregates prepared from NaOH treatment on commercial nanoparticle P25 can be regulated by adjusting either the treatment temperature or the concentration of neutralization HCl solutions. The function of the NaOH treatment is to convert the starting TiO₂ particles into sheets composed mainly of anatase phase that is more feasible for rolling of the sheets to form nanotubes. The treatment temperature determines the extent of precursor conversion, which eventually influences not only the pore structure of the nanotube aggregates but also the structural stability of

crystalline anatase at high temperatures. The process of TiO₂ sheets rolling into nanotubes upon acid washing to remove electrostatic charges has been confirmed by the TEM study in the present work. Both the charge-removing rate and equilibrium state of the electrostatic charges on TiO₂ affect the final structure of the aggregates. This indicates that the size of formed nanotubes can be regulated or modified by rinsing at different pH values, using NaOH or HCl of different concentrations. The nanotube TiO₂ exhibits a higher activity as a catalyst support than the nanoparticle P25 in NO reduction with NH₃, indicating that the vast surface created from the hydrothermal alkali treatment is accessible to the reacting molecules.

Acknowledgment. This research is supported by the National Science Council of Taiwan (NSC 92-2214-E-006-021) and NCU-ITRI Joint Research Project of National Central University (NCU-ITRI 930202).

CM049643U